Accident Analysis and Prevention 45 (2012) 305–316

Contents lists available at ScienceDirect

Accident Analysis and Prevention

journal homepage: www.elsevier.com/locate/aap

Fuzzy-logic-based network for complex systems risk assessment: Application to ship performance analysis

Seraphin C. Abou *

Mechanical and Industrial Engineering Department, University of Minnesota Duluth, 1305 Ordean Court, Duluth, MN 55812, USA

ARTICLE INFO

Article history:
Received 7 March 2011
Received in revised form 21 July 2011
Accepted 24 July 2011

Keywords:
Diagnosis
Fuzzy systems
Marine engineering
System safety
Uncertainty analysis

ABSTRACT

In this paper, a new interpretation of intuitionistic fuzzy sets in the advanced framework of the Dempster–Shafer theory of evidence is extended to monitor safety-critical systems' performance. Not only is the proposed approach more effective, but it also takes into account the fuzzy rules that deal with imperfect knowledge/information and, therefore, is different from the classical Takagi–Sugeno fuzzy system, which assumes that the rule (the knowledge) is perfect. We provide an analytical solution to the practical and important problem of the conceptual probabilistic approach for formal ship safety assessment using the fuzzy set theory that involves uncertainties associated with the reliability input data. Thus, the overall safety of the ship engine is investigated as an object of risk analysis using the fuzzy mapping structure, which considers uncertainty and partial truth in the input–output mapping. The proposed method integrates direct evidence of the frame of discernment and is demonstrated through references to examples where fuzzy set models are informative. These simple applications illustrate how to assess the conflict of sensor information fusion for a sufficient cooling power system of vessels under extreme operation conditions. It was found that propulsion engine safety systems are not only a function of many environmental and operation profiles but are also dynamic and complex.

1. Introduction

In today's modern society, the safety, availability, reliability and *high performance* of marine transportation systems have become increasingly important so as to minimize catastrophic events. The risk analysis of these safety-critical systems concerns "risk assessment" and "risk management," where the former generally involves objective elements and the latter involves both objective and subjective elements. From various safety perspectives, maritime safety systems (a class of systems with "*low frequency and high consequences*") deal with the monitoring, detection, predictive trending and accommodation of engine degradation and its faults and failures. While management and engineering actions have a significant impact on the reliability of marine transportation systems, these factors have received too little attention in the evaluation of critical risks at the system level. For the rapid and condition-based risk management of marine propulsion systems, it is essential to have a safety system and reliability analysis methods that can integrate analyses across physical scales and interface models and data from multiple fields of science and engineering smoothly to quantify system-level risk.

In this paper, technologies addressing safety improvement and the monitoring of engine performance monitoring issues are presented. Fig. 1 depicts a general architecture representing the integration of marine systems health assessment and control. Proactive health monitoring and diagnostics based on advanced neural network and fuzzy logic technologies will alleviate service and in-operation damage problems.

Formal safety assessment methodology takes into account detailed information about system states and accident characteristics and provides quantitative risk estimation. However, one of the major problems continually facing operators of pod-equipped cruise ships is that of main failure, which can be classified into two types: (1) failure in mechanical components and (2) failure in electrical components. Moreover, the electrical failures can be classified as either burning of the coils of the stator, failure of power supply cables causing short circuits, loss of control of the motor speed, and loss of the transmission of the electrical power. The proposed approach to monitor engine health draws from methodologies and processes employing both physics-based and empirical techniques derived from a wide range of engine system disciplines, including materials, structures, and controls. According to Benitez-Perez et al. (Elishakoff, 2004), conventional risk models are event-based models, such as event trees and fault trees, where the system accident is the end state of a cause-effect sequence stemming from a deviation caused by a failure event such as component failure, human error, or external disturbance. However, from these models,

* Corresponding author. Tel.: +1 218 726 8250; fax: +1 218 726 8185.
E-mail address: sabou@d.umn.edu

0001-4575/$ – see front matter © 2011 Elsevier Ltd. All rights reserved.
doi:10.1016/j.aap.2011.07.017

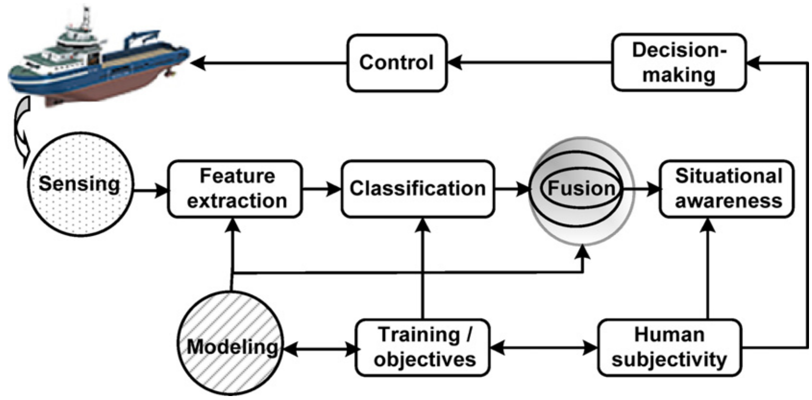

Fig. 1. Diagnostic and decision-making process.

the information pertaining to sensors' data fusion is rarely known with complete confidence; it is often random, vague, and imprecise. Recently, Lisnianski et al. (2000) and Aksu and Turan (2007) defined basic concepts of multi-state system (MSS) reliability. They make the point that reliability can be increased not only by employing contrasting methodologies but also by creating several stages within a methodology.

To extend the current state of the art of system health monitoring models in general, and of Dempster–Shafer evidence theory (DST) in particular, this study presents mathematical operations using intuitionistic fuzzy values as the operations on belief intervals including the following: (*i*) probability theory (Elishakoff, 2004), (*ii*) fuzzy set and fuzzy logic theory (Alfaro-Cid et al., 2001), and (*iii*) Dempster–Shafer evidence theory (Yager, 1983). Each of these theories maintains its own views and often focuses on one aspect of uncertainty. Therefore, given the many performance evaluation factors, it is common sense that system safety practices in complex systems applications recognize key issues to be addressed in hazards assessment, as follows:

- How do we go about finding effective risk controls and management mechanisms?
- What do we have to know in this study, for example, about the cavitation of the ship hull or blade surface damage to control it?

Because the primary goal of this paper deals with engine diagnosis and risks from critical failures, we assume the propulsion system to be a multi-state system (MSS) (Kahneman, 2002), thereby facilitating its formulation. Indeed, we have in a previous study, intended to transform an MSS reliability analysis into a set of two states of reliability analysis (Abou, 2010), (Abou et al., 2007). The theory presented is consistent with the MSS principles described by Lisnianski et al. (2000). However, the problems of MSS analysis are generally much more complex than the problems of analyzing the reliability of two states. For instance, with a widely used assumption in the analysis of two system states (Henley and Kumamoto, 1980; Holtrop (Wang et al., 1995); Sauer et al., 1991), an exponential distribution cannot be assumed for the reliability function $R_i(t)$, for all $i = 1, 2, 3, \ldots, m$. In fact, under Markov-based models for analyzing system reliability, the function $R_i(t)$ has a complex form, developed by Lisnianski et al. (2000). Analogous to the human brain, the diagnostic and decision-making structure illustrated in Fig. 1, is used to apply the performance evaluation of multi-sensor data fusion to marine transportation systems and real data. The human brain routinely carries out information gathering and fusion. Although data-driven methods and the Dempster–Shafer evidence theory are great for reliability analysis, risk assessment results obtained from these methods generally lack information regarding the nature of the damage and severity. The imprecision in probabilities and utilities can be modeled as intuitionistic fuzzy sets through membership functions defined for the sets of possible probabilities and utilities (Atanassov, 1999), (Barnett, 1981), (Szmidt and Baldwin, 2003), (Szmidt and Kacprzyk, 1996).

The purpose of this study was not simply to create fuzzy nets that relate propulsion engine dynamics; we also need the nets to be reasonably accurate and safe and to cover their distributed functionality knowledge, even under inclement weather conditions. From different perspectives, we carefully analyzed critical situations that may impair ship safety. We made use of intuitionistic fuzzy sets for the adequate representation of quantitative data to deal with the inherent uncertainty and reasoning of the information resulting from inappropriate data collection.

Following these introductory remarks, the next section presents the definition of the problem and the theoretical formulation methods for the analysis of uncertainties. The following section introduces alternative approaches that exist in the literature for building a frame of discernment and for addressing uncertainties at each step to collect observations from various similar or dissimilar sources and sensors. The paper is organized in such a way as to stress the following fundamental considerations: after a brief description of the overall dynamics of the system proposed by Aksu and Turan (2007), the paper presents the analysis of probable incipient faults acting on the system on the basis of the so-called evidence frame of discernment (Shafer, 1976; Yager, 1983; Wang et al., 1995).

These accepted methods for the classification of faults are used in this paper to enhance the evaluation of their severity and monitor the associated risks. Then, the state space reconfiguration that extends the Dempster–Shafer evidence reasoning strategy is used to assess the sensors' sensibility. The plausibility of and belief in fused information provided by sources is weighted to predict incipient faults in engines. The illustrative case study discussed in Section 6 reveals the accuracy of the proposed fuzzy model.

2. Definition of the problem and method

Ship structures differ from other engineering systems primarily in terms of their dynamic environment. To conduct risk analysis in marine transportation systems at both the system and component levels, several steps are required. While diagnostics are used to investigate or analyze the cause or nature of a condition, situation or problem, prognosis is used to gain knowledge ahead of time, to calculate or predict the future as a result of rational study and analysis of available pertinent data; in general, the risk evaluation of complex systems consists of a data acquisition system, signal

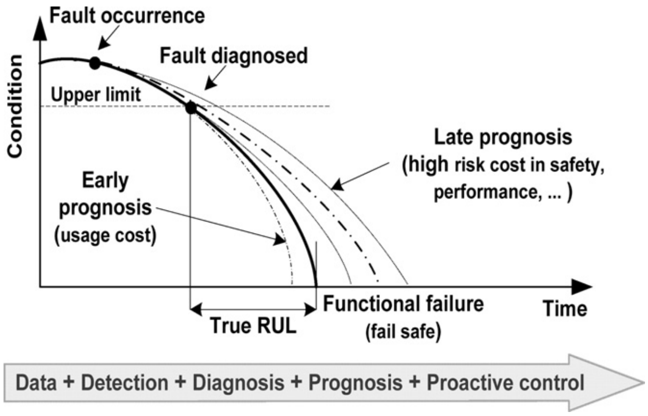

Fig. 2. Event detection/health monitoring process.

processing, feature extraction and selection, physical models and knowledge of damage when possible.

Information processing and fusion are used to collect observations from various similar or dissimilar sources and sensors, extract the required information (inferences) and combine/fuse these to obtain enhanced understanding of the status and to identity a perceived pattern. This process is crucial for marine systems and can be termed multi-source multi-sensor information fusion. In general, the process encompasses the concept of estimating useful life (RUL) of a component or system (Fig. 2).

Because marine transportation systems encompass "*single failure*" components, the idea of making use of the extension of the definition of intuitionistic fuzzy sets is relevant in real life and derives from positive (independent) and negative information that lies at the core of intuitionistic fuzzy sets. For example, intuitionistic fuzzy set is well known in psychology and soft computing technologies. Because the risk assessment of a safety-critical system uses large amounts of data from sensors, it would be difficult to deal with machine learning (making use of examples and counter-examples), modeling of preferences, or voting without taking into account positive and (independent) negative data. Given this information, user or control systems may be capable of proactively adapting their use or mission to complete mission goals and/or extend the RUL (Fig. 2).

A typical electric propulsion system (consisting of, for example, a synchronous generator, power transformer, frequency converter, synchronous/inductive motor, controller, propeller, and other load demands, such as pumps, winches, lighting) is shown in Fig. 3. From a system safety perspective, the integrated architecture of Fig. 3 combines a propulsion system and ship service electrical system into a single power system.

Conceptually, vessels with integrated propulsion systems are similar to hybrid electric automobile systems; components such as the hull, the main engine, and the propeller are in various stages of development to achieve full-scale torque levels. Regarding the propeller, the propulsive efficiency is a function of the pressure produced by different propeller blade shapes. Indeed, not equipping these systems with proper safety and protection features can have various unexpected consequences, including operation failure or a breakdown of components or even of the entire system. In fact, the loss of propulsion or a complete blackout of the entire vessel is frequently among the most common consequences of omitting proper risk controls and management systems.

For example, if we want to know whether a specific latent fault exists in the propulsion engine, the idea is to build a frame of discernment defined as $\aleph = \{e, -e\}$, which would describe the state of the engine to be either faulty e or healthy $-e$. The demand for expansion of the performance envelope of mobility structures of

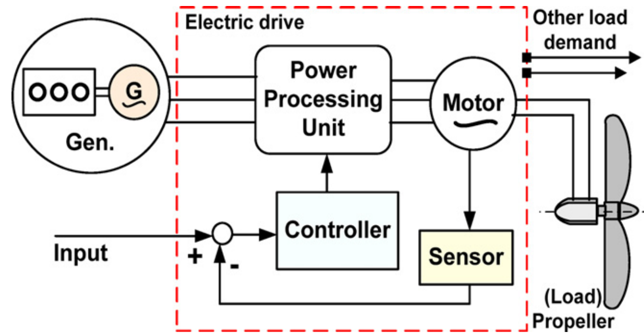

Fig. 3. Integrated electric propulsion system scheme.

ships, such as ever-increasing speeds while enforcing stability, has generated significant advances in the development of more flexible and, consequently, more complex and nonlinear systems. However, for complex propulsion systems, computational advances still fall short for many reasons. Furthermore, the potential of using modeling and simulation to understand innate system behavior under unforeseen failure scenarios in inclement weather becomes highly inefficient. Therefore, the research question in this study may be formulated as follows:

If we want to maximize diagnostic performance and accommodate more faults and associated risks so that data fusion can be used at the feature and decision levels, for instance, $\aleph = \left\{\varepsilon_0, \varepsilon_1, \varepsilon_2, .., \varepsilon_{h-1}, \varepsilon_h\right\}$, *to what extent can the frame of discernment be expanded*?

In this context, ε_0 would signify the absence of faults, and ε_i would signify the presence of the ith fault. It is important to stress the point that the ability to detect an impending failure in propulsion a mechanical power system at an early stage when expensive and possibly catastrophic system failures can be prevented is a crucial concern of this study. It is known that the generic configuration of a pod propulsion system consists of steerable and fixed pod units. Mechanical, electromechanical, electronic, and electrical components have been incorporated into the spectrum analysis of reliability assessment along with their associated failure and repair rates. Hydraulic motors and driving gears power the cog wheel for rotation. Then, this motion is transmitted to the thrust components. As part of the propulsion system, the mathematical model of the motor torque is presented in Appendix A.1.

Based on the proposed approach, because safety is viewed as a dynamic control problem rather than a reliability problem, any appropriate use of a given uncertainty formulation in decision making under uncertainty may lead to the selection of a suitable alternative using a "*valuation function*." The determination of *the valuation function* depends on the payoffs of various criteria involved and knowledge of experts about the state variable. The decision-making problem becomes more complex when multiple sensors that have different levels of sensibility concerning the data being collected are involved. Moreover, their model will reflect the knowledge of the state or value of the payoffs.

Therefore, we established the idea that accidental events result from a lack of enforcement of safety constraints. Thus, the approximate error $h(x, \upsilon)$ in Eq. (A5) (Appendix A.1) is assumed to be "fuzzy," whereas the knowledge about the state $x(t)$ represents a *belief function*, and the control signal u determines the optimal control method (Gabasov and Kirillova, 2006). Accordingly, the computation algorithm used to resolve this problem is part of a class of stochastic search algorithms. It is very effective in finding near-optimum solutions to problems where an exhaustive search is impractical or where there is no algorithmic means of finding a solution.

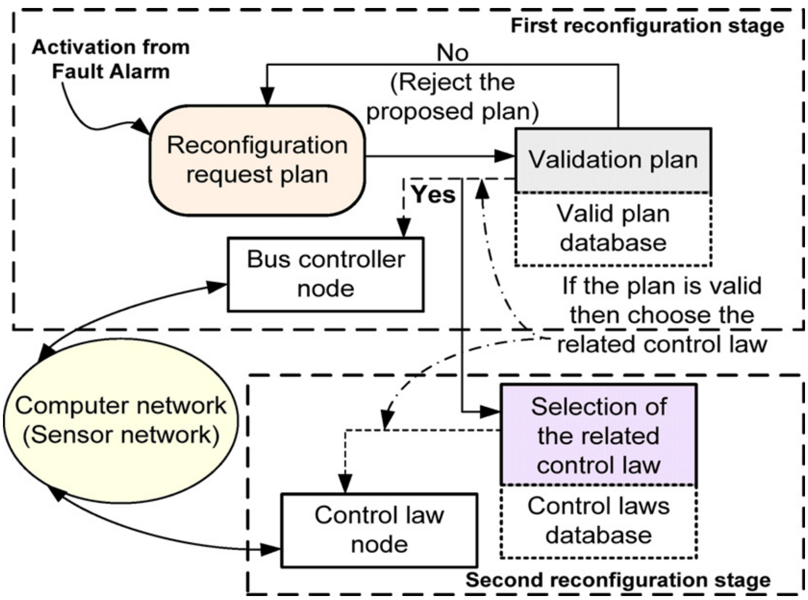

Fig. 4. Structure of the reconfiguration system.

3. Risk in the frame of discernment

Since the Maritime Safety Committee (MSC) initiated the Formal Safety Assessment (FSA) in 1993, remarkable efforts have been made at different levels (e.g., systems, subsystems, and operational and organizational levels) to achieve a safe maritime transport system (MTS). However, the application of the FSA to the safety of ships, including high-speed passenger catamaran ferries, bulk carriers, and other kinds of vessels, is not a panacea that can prevent the occurrence of accidents and failure incidents at sea. As a method that supports decision making for maritime legislation, the FSA offers more rational safety guidelines than the traditional "Regulation by Disaster" method. Compared to other assessment methods, safety principles derived from the FSA are more formal, reasonable, and integrated. They can be applied to the analysis and evaluation of both the actual hazard after an accident has occurred and the potential "what would go wrong" scenario (e.g., latent failure) before an accident occurs.

We define risk not only as the potential for system failure but also as the lack of knowledge and aggregation of information about a system's states that would result in losses, while Yager defines decision making under uncertainty as a class of decision problems where different manifestations of state variables $[X(t)] = [x_1, x_2, ...x_n]^T$ lead to different payoffs (Yager et al., 1994).

It is important to know that the major issue we face is the representation of knowledge concerning state variables: $[X(t)] = [x_1, ..., x_n]^T$. Therefore, to set up a frame of discernment, one of the important steps we used was to define the objects around which the evidence reasoning process is to take place. In this sense, diagnosis objects and the corresponding fault frame of discernment are evaluated. Elements in the frame of discernment can represent the diagnosis hypothesis. However, a literature review spanning (Safranek et al., 1990), (Barnett, 1981), (Carter et al., 2001), and (Szmidt and Kacprzyk, 2005) shows that different hypotheses correspond to different requirements for measurements and methods of measurement processing and, hence, may lead to different frames of discernment. We believe Barnett (Atanassov, 1999) is the first researcher who pointed out that an indiscriminate use of Dempster's rule in combining evidence requires an exhaustive enumeration of all subsets or supersets of a given set in the frame of discernment, which as an exponentially complex process, makes the rule computationally intractable when large frames of discernment are involved. Barnett also suggested a way avoid this computational difficulty and provided a consideration of singleton hypotheses and their negations. We refer interested readers to (Safranek et al., 1990; Barnett, 1981; Carter et al., 2001; Szmidt and Kacprzyk, 1996; Kahneman, 2002; Atanassov, 1999; Sugeno, 1974).

We decided to develop, in this study, knowledge of system behavior and information that pertains to various sensors' data based on the Dempster–Shafer evidence theory and extend its frame of discernment. This approach commonly includes three steps (Shafer, 1976): (1) *evidence representation using an evidence structure for each information source*, (2) *combination of evidence structures*, and (3) *decision making based on the combined evidence structure*.

For instance, suppose that a propulsion engine suffers from one or more of two faults, α_1 *and* α_2. A frame of discernment in this case can be formulated as follows: $U = \{\alpha_1, \alpha_2\}$ and $\left\{\varnothing, \alpha_1, \alpha_2, (\alpha_1, \alpha_2)\right\}$. Then, by allowing a general formulation of (2), $\aleph = \left\{\varnothing, \alpha_1, ..., \alpha_{h-1}, \alpha_h\right\}$ is a frame of evident discernment, and 2^n becomes the power set composed of all possible subsets of $\aleph$. All the classes in $\aleph$ are assumed to be mutually exclusive and exhaustive. Next, after the frame of discernment is determined, we must define a *mass function* f_m as a mapping of a power set $\Gamma(\aleph)$. Let a function $f_m : \Gamma(\aleph) \to [0, 1]$ be a *mass function* or *the basic probability assignment function*:

$$\begin{cases} \sum_{U \subseteq \Gamma(\aleph)} f_m(U) = 1 \\ f_m(\varnothing) = 0 \end{cases} \tag{1}$$

f_m expresses the proportion of all relevant and available evidence that supports the claim that a particular element of $\aleph$ belongs to the set U but to no particular subset of U. A subset U with non-zero mass in Eq. (1) is called a *focal factor*: a crisp set consisting of all focal factors of an object to be judged. Focal elements and their masses form an *evidence structure* (*also referred to as belief structure*), expressed as

$$\{(U, f_m(U)) | U \subseteq \aleph, f_m(U) > 0\}; \; U = \{u_i | i = 1, 2, \ldots, n\},$$

where n is the number of focal factors. $(U, f_m(U))$ is referred to as a piece of evidence.

Even though we knew from risk assessment and controls perspectives that ship engine components can be organized into two classes, *controlling and controlled components*, obviously none of these core structures operate in a vacuum. For example, the *critical impact forces* event and the *emergency anchoring failure* event are both dependent on the *critical weather force* event. On the other hand, the *critical weather force* event may be dependent on the *critical drifting direction* event. These multiple interactions make it difficult to know how to fuse decisions that are derived based on multi-sensor data, which can be imprecise and sometimes conflicting (Fig. 1). In the information fusion process, the degree of belief held by an observer regarding a certain fault is determined by the mass function f_m. It is known that different information or evidence can produce different degrees of belief with respect to a given fault. *Dempster's rule*, which combines independent evidence, satisfies the following condition:

$$\oplus_{i=1}^{n} f_{m_i}(U) = \begin{cases} \dfrac{1}{1-\delta} \displaystyle\sum_{\cap_{i=1}^{n} U^i = U} \prod_{i=1}^{n} f_{m_i}(U_i), & \text{if } U \neq \varnothing \\ 0, & \text{if } U = \varnothing \end{cases}$$

with

$$\delta = \sum_{\cap_{i=1}^{n} U^i = \varnothing} \prod_{i=1}^{n} f_{m_i}(U_i) \quad > \quad 0 \tag{2}$$

where $\oplus$ denotes the combination operator; U_i designates the focal in source I; $f_{m_i}(U_i)$ is the corresponding mass; $\cap_{i=1}^{n} U_i$ denotes the intersection of focal U_i through U_n ; and δ represents a measure of conflict among the sources to be combined. It is important to note that $f_m = f_{m_1} \oplus f_{m_2}$ represents the combination of f_{m_1} and f_{m_2} and carries the joint information from the two sources. This property of evidence combination satisfies the commutative and the associative relationships as follows. This property deviates from traditional practice, provides a rigorous framework, and can be used to mitigate or control hazards and safety related constraints:

$$\begin{cases} f_{m_1} \oplus f_{m_2} = f_{m_2} \oplus f_{m_1} \\ (f_{m_1} \oplus f_{m_2}) \oplus f_{m_3} = f_{m_1} \oplus (f_{m_2} \oplus f_{m_3}) \end{cases} \tag{3}$$

Once this high level of evidence combination is attained, the uncertainty model, which unfortunately does not naturally support the direct integration of human operators in the fault detection process, will be taken into account. As a result, the interesting capability of describing vague and imprecise facts and working with the system when precise information is not available makes fuzzy logic a powerful tool in this case. In this sense, we use evidential measures including *belief*, *plausibility*, and *pignistic probability* for decision making. More importantly, to deal with fuzziness in data, a generalized evidential reasoning framework is used by replacing focal factors that may make the analysis very complex with fuzzy sets. Accordingly, the *fuzzy evidence structure* is formulated as follows:

$$\psi_s = \left\{ (\tilde{U}, f_m(\tilde{U})) \,\middle|\, \tilde{U} \subseteq \aleph \right\}$$

where $\tilde{U}$ is a fuzzy set and $(\tilde{U}, f_m(\tilde{U}))$ is referred to as the piece of fuzzy evidence. Dempster's combination rule in Eq. (1) can be generalized directly by replacing U and U_i with the fuzzy sets $\tilde{U}$ and $\tilde{U}_i$.

The generalized evidential reasoning framework is embedded in the block diagram shown in Fig. 4. It broadly describes the principle of the intelligent diagnosis process. The effectiveness and the interrelated functions of each block depend to a large extent on how redundant and complementary information cues are obtained from the sensors. By effectiveness, in terms of fault resilience, we mean the extent to which the system outputs related to safety

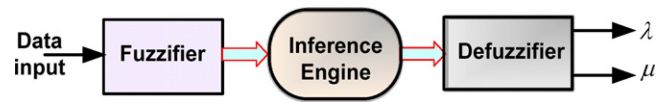

Fig. 5. General structure of the fuzzy Block.

requirements integrity are sufficient and comply with the necessary risk reduction level (ALARP) and the priority needs of a single safety-related subsystem.

In addition, notions such as belief, plausibility, and pignistic probability are generated to deal with fuzzy evidence for decision making. More importantly, it is decided at which level of abstraction the fuzzy evidential analysis process is to take place (i.e., at the measurement level, at the feature level, and/or at the decision level). We noticed that the fuzzy abstraction level setting is in accordance with the first class of faults that is considered, or "*faults that are related to propeller pitch measurement and the engine cooling system effectiveness*." Thus, the proposed criterion can be used to characterize the membership function F, which might associate each member of a set of values in the interval [0,1], as follows:

$$\begin{cases} \mu_F : \quad X \to \quad [0,\ 1] \\ F = \left\{ (x, \quad \mu_F(x)) \,\middle|\, x \in X \ \text{ and } \ 0 \le \mu_F(x) \le \quad 1 \right\} \end{cases} \tag{4}$$

For those dynamic systems described by state models with inputs and outputs, the general structure of the fuzzy block is shown in Fig. 5.

Besides extending the conventional Dempster–Shafer theory to the new interpretation of intuitionistic fuzzy sets in the advanced framework of discernment, we would like to improve the predictive monitoring strategy and compute the future control sequence following the optimal one-step-ahead prediction principle because the system output $y(t+i|\,t)$ may be driven close to $y(t+i)$ for the predicted horizon. This strategy is defined in the observed system (Fig. 5) as the following linear representation:

$$\begin{cases} \left(1 + a_1 z^{-1} + .. + a_{na} z^{-na}\right) y(t) = \\ = z^{-d}\left(b_0 + b_1 z^{-1} + .. + b_{nb} z^{-nb}\right) u(t-1) + \\ + \left(1 + \varepsilon_1 z^{-1} + .. + \varepsilon_{n\varepsilon} z^{-n\varepsilon}\right) e(t) \end{cases} \tag{5}$$

where $[a_1 \ .... \ a_{na}]$, $[b_0 \ ..... \ b_{nb}]$, and $[\varepsilon_1 \ .... \ \varepsilon_{n\varepsilon}]$ are coefficients related to the system output, system input, and system output variables error, respectively.

The appropriate way to manage the system state conditions in Eq. (5) is to implement an objective function J that depends on present and future control signals and uncertainties. We study the objective function described as follows:

$$J(n_0, \quad n_1) = \sum_{j=n_0}^{n_1} \delta(j)\left(\hat{y}(t+i|\,t) - w(t+j)\right)^2 + \\ + \sum_{j=n_0}^{n_1} \lambda(j)(\Delta u(t+j-1))^2 \tag{6}$$

where n_0 and n_1 are the minimum and maximum costing horizons, $\delta(j)$ and $\lambda(j)$ are weighting sequences, and $w(t+j)$ is defined as the future trajectory to be followed. The objective function (12) is involved in the optimization of the future control response $u(t+j)$, where the entire propulsion system response $y(t+j)$ is closed to $w(t+j)$. In most cases, for this objective function, knowledge regarding the exact forms of all limiting functions to determine optimal solutions is not required.

4. State space reconstruction and Dempster–Shafer framework

Conventional information fusion architectures are challenged by developments in sensor networks that allow individually owned (and thereby selfish) sensors to interact and share data. Various techniques, such as the extended Dempster–Shafer framework of discernment and computational mechanism design, allow for the development of engineering networks with desirable system-wide properties. In this process, sensors are represented as selfish rational agents, each attempting to fulfill their own individual goals.

Much attention has been devoted to multi-source multi-sensor information fusion as a discipline. This technique is finding ever-increasing applications in biomedical, industrial automation, aerospace systems, and environmental engineering. However, in some applications, each sensor may be individually owned by different stakeholders. In such cases, sensors may operate in a competitive rather than cooperative environment, and thus, they may attempt to optimize their own gain from the network at a cost to the performance of the entire system. Therefore, to properly describe the uncertainties arising from measurement noise, modeling error, and data incompleteness, knowledge about possible faults in the system illustrated in Fig. 5 can help develop a power set $\Gamma(\aleph)$ of fault occurrence. Each element in the power set has a value that differs from the one given by the basic probability assignment function. The number of a power set elements is 2^n (n is the number of elements of the frame of discernment), considering n types of faults and k sensors. Using the information provided by the sensors, let $X=[x_1\ x_2\ ..\ x_n]$ be the state variables of the propulsion engine of the vessel as follows:

$$\begin{bmatrix} x_1 \\ . \\ . \\ x_n \end{bmatrix} = \begin{bmatrix} x_{11} & . & . & x_{1n} \\ . & . & . & . \\ . & . & . & . \\ x_{n1} & . & . & x_{nn} \end{bmatrix} \tag{7}$$

where x_i is the ith feature that describes a specific aspect (fault or state) of the engine and n is the number of features (states or types of faults including the fault-free state).

For simplicity, the extension to generalized decision rules that is provided in this paper is restricted to settings where the space of the inputs has essentially the same characteristics as the space of outcomes. The system's *performance-oriented criteria analysis* supports primarily a set of environmental and operational scenarios chosen to be as realistic as possible, including the full scale of measurements of the propulsion power, ship speed, wind speed and direction, sea and air temperature, and different loading conditions. A fuzzy logic prediction model is helpful in this regard (Benitez-Perez et al., 2006). Because it is costly to obtain a high level of evidence, a literature review shows that users minimize the need for it by maximizing the assurance for both the existence and evaluation accuracy of other sources (e.g., experts) (Henley and Kumamoto, 1980; Murchland, 1975).

In general, such assurances may vary in strength from one to another in terms of measurement context. The challenge is that of calculating the basic probability assignment f_m, (the m-function, Shafer, 1976) based on the extracted feature (faults) vectors (1). The fundamental difference between m-functions f_m and probabilities is that probabilities are assigned to individual elements of a frame of discernment, say $\aleph$, whereas m-functions f_m are assigned to a subset of the frame of discernment. A fuzzy measure μ_Γ defined on a measurable space (X, A) is a set of functions denoted $\mu_\Gamma : \Gamma(\aleph) \to [0, 1]$ satisfying the following conditions:

$$\begin{cases} \mu_\Gamma(\varnothing) = 0 \text{ and } \mu_\Gamma(X) = 1 \\ \forall (A, \quad B) \big| B \in A, \text{ and } A \subseteq B \\ \text{imply } \mu_\Gamma(A) \le \mu_\Gamma(B) \end{cases} \tag{8}$$

where (X, A, μ_Γ) is said to be a fuzzy measure space.

It should be noted that such a "*feature space*" is generally not unique, nor may it even be possible to express particular dynamic evolutions under a specific model. However, we have flexibility in the choice of model class, parameter regimes, embedding approach, etc., to provide "*local*" uniqueness regarding the information for a specific application of the method. Therefore, we seek to define the general criteria of the model representation related to the data classes of interest, such as local parameter continuity (phase space evolutions which, being topologically "*close*" are also "*close*" in the coefficient space) (Haimes, 2004). Another important parameter in this analysis is sensor location. Therefore, the distance between objects (e.g., sensors) k given by the kth row of a $m \times n$ data matrix and fuzzy cluster centers become a base step of pattern recognition.

Yang and co-workers (Wang et al., 1995) recently attempted to address this issue. They presented a neural network approach for the diagnosis of complex dynamic systems based on multi-sensor and multi-domain knowledge fusion. On the contrary, in Dempster–Shafer evidence theory, we do not assign any degree of belief to the empty proposition and we ignore the possibility for an uncertain parameter to be allocated outside the frame of discernment. On the other hand, using fuzzy sets theory enables uncertainty modeling when historical data are not available for analysis. The method facilitates uncertainty analysis when the uncertainty arises from lack of knowledge or "fuzziness" rather than randomness alone.

Therefore, rather than provide a simple probability for the events, through the implementation of an advanced frame of discernment, novel events can be conceived, for instance, using the free space ultimately left by a residual event. Thus, we focused on ensemble classifiers as the main feature-level data fusion approach and inference engines as the decision-level data fusion approaches. Fig. 6 shows a sample architecture for data fusion based on the distinction between feature-level and decision-level fusion. Similar analysis for multi-sensor fusion and integration focusing on sensor technology development is performed for various applications, such as robotics, biomedical and equipment monitoring.

It is important to note that data-driven methodologies can only provide part of the information required to develop effective diagnostic systems. To maximize knowledge discovery, data-driven techniques must be fused with physics-based models of the structure under analysis that include disturbances (e.g., temperature, noise, vibration) from sensor locations. However, because different methods of measuring the distance between sensors result in diverse solutions for failure recognition, for simplicity, and without the loss of generality, we consider the Minkowski distance in the spatial location and the measurement process as follows (Groenen and Jajuga, 2001):

$$d_{kj} = \left[\sum_{k=1}^{m} \left(s_{ki} - x_{ij} \right)^{\alpha} \right]^{1/\alpha} \tag{9}$$

where s_{ki} is the ith element of the measurement vector A_{sk} collected on the kth sensor; x_{ij} is the ith feature of the jth fault; and d_{ki} is the distance between A_{sk} and the feature vector X_{ij} describing the jth fault or engine state. When α equals 2, the Minkowski distance is reduced to the well-known Euclidean distance; on the other hand, if $\alpha = 1$, the distance converges to the corner distance.

An interesting impact of this result arises because we do not use decision rules that depend solely on a single criterion. In these common settings that use a polynomial form of order less than or equal to $(2n_k - 1)$, the one-dimensional Euclidean formula, which is a well-known numerical integration technique, yields the exact integral for any function. It should be noted that various forms of the Minkowski distance expression do not account for the metric

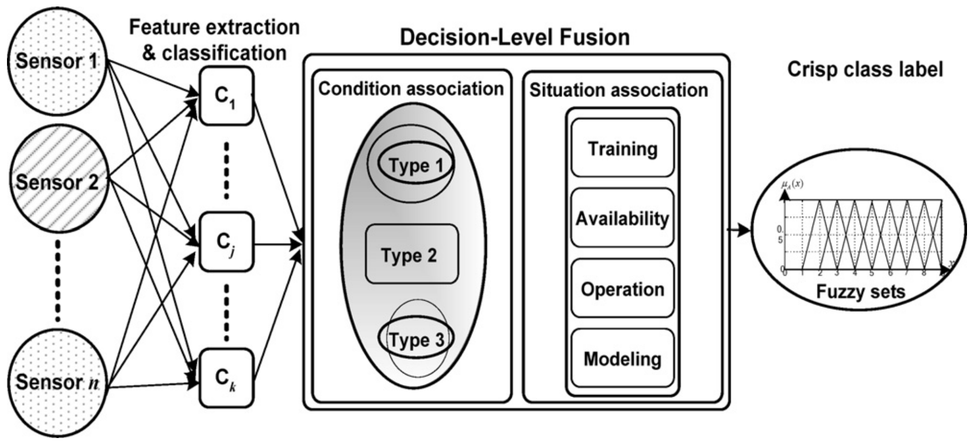

Fig. 6. Architecture for data fusion. (a) Sensor (1) and (2) data inconsistency. (b) Sensor (3) and (4) data inconsistency.

variability of individual coordinates. Moreover, *the smaller the distance* d_{ki} *is, the more probable that the* ith *fault* information from Kth sensor s_k can be determined.

Consider the approximate error $h(x, \upsilon)$ in Eq. (5) for the entire rule r_i:

$$\begin{cases} h_i(x_j) = \mu_1^i(x_1) \otimes \mu_2^i(x_2) \otimes .. \otimes \mu_s^i(x_s) \\ \otimes : [0, 1] \times [0, 1] \to [0, 1] \end{cases} \tag{10}$$

The algebraic product of Eq. (17) is

$$h_i = \prod_{j=1}^{s} \mu_j^i(x_j) \tag{11}$$

where $\mu_j^i \in \tilde{U}_i$ are fuzzy sets defined in the antecedent space, $x_j \in \mathbb{R}^n$ stands for the current state measures vector, s is the state number, $u \in \mathbb{R}^m$ denotes the control input, $i = 1, ..., n$ is one of the fuzzy rules, n is the number of the rules, which is equal to the number of possible component faults, and μ_j^i are the related Gaussian fuzzy set membership functions.

Implicitly, the extension of the frame of discernment adopts an algorithmic view of intelligence. However, inadequacy of statistical estimation of spurious faults may result in the imprecise and unreliable synthesis of risk factors. To avoid this problem, a Euclidean vector space (i.e., a class of "*feature space*" classifier) is used to construct the most general statistical measure directly from data observations of a vessel engine. Therefore, an approximation of the j -dimensional integration by the full-tensor product $\otimes$ of the one-dimensional Gauss–Legendre quadrature can be formulated as

$$\begin{cases} \mu(u(t, \xi)) = \displaystyle\int_{\Omega} u(t, \xi) w(\xi) d\xi \\ = \displaystyle\sum_{i=1}^{n_k} .. \sum_{i=1}^{n_k} u(t, \xi_1 ... \xi_{i_k}) \times w_1 \otimes .... \otimes w_{i_k} \end{cases} \tag{12}$$

The identification of fuzzy decision factors is normally required to provide for a significant degree of performance assessment of complex systems and to ensure safe operation under uncertain conditions.

5. Fuzzy decision factors and rules

According to the above classification, the method of evaluating safety conditions of maritime safety systems has two aims:

- Theoretical—recognition of safety attributes, their characteristics and temporal changeability
- Practical—analysis of what kind of results we are able to achieve from theoretical recognition and what we can say about technological influence on the system and public safety.

To illustrate this, a global treatment method that involves three sources of vagueness (*randomness, fuzziness, and errors*), has been proposed and is taken into consideration in the risk assessment process. We identified two ways of obtaining m-values (mass function) in this framework:

(1) they may be assigned directly by the decision maker on the basis of subjective judgment, or
(2) they may be derived from a compatibility relationship between a frame with known probabilities and the frame of interest.

Because model tests were not available, the problem was resolved in this study by calculating the theoretical propulsion power efficiency under real-time conditions using standard empirical resistance and the propulsion methods proposed in (Harvald, 1983) and (Holtrop, 1984). As a result, the decision-making tool and calculation by empirical methods, even with carefully prepared data, are far from accurate and only account for physical features in restricted navigation areas. At each time instant, the fault information s_{ki} (i.e., the ith measurement) is read from the kth sensor. The outputs of each faulty fuzzy model are computed, as is the distance d_{ki} between elements of the measurements vector A_{sk} and the feature vector X_{ij} describing the jth fault or engine state (9). Furthermore, once the basic probability function is obtained, the final *m-value* function f_m is computed as follows, using combination rules (2) and (8):

$$\begin{cases} p_{m_j} = [d_{ij}^{-1}]; \displaystyle\sum_{j=1}^{n} p_{m_j} = 1; \quad j = 1, \quad 2, \quad ....., \quad k \\ f_m = p_{m_1} \oplus p_{m_2} \oplus ..... \oplus p_{mk} = f_{m_1} f_{m_2} .... f_{mk} \end{cases} \tag{13}$$

$$f_{m_j} = \frac{\prod_{j=1}^{k} p_{mj}}{\left(1 - \sum_{i=1}^{n} \prod_{j=1}^{k} p_{mj}\right)} \tag{14}$$

From the final *m-value* function assignment f_m, the fundamental consideration defines the *upper* and *lower bounds* of the fault belief interval. This interval contains the precise probability of a set of interest (in the classical sense) and is bounded by two non-additive continuous measures called the *Belief function Bel*(.) and *Plausibility function Pl*(.). The lower bound *Belief function* represents the minimal support for a set a and can be interpreted as a global assessment of one's belief that hypothesis a is true. The upper bound *Plausibility* *function* expresses the greatest potential degree of belief in a. The relationship between the *Plausibility function* $Pl(.)$ and *Belief function* $Bel(.)$ is as follows (Yager, 1983):

$$\begin{cases} Bel(a) = \sum_{b \subseteq a} f_m(b), & \forall a \subseteq \aleph \\ Bel(\varnothing) = 0 \quad \text{s} \quad Bel(\aleph) = 1 \\ Pl(a) = 1 - Bel(\tilde{a}) = \sum_{b \cap a \neq \varnothing} f_m(b) \end{cases} \tag{15}$$

It should be noted that the *Belief function* formalism may be explained in many ways. Although not the most rigorous, in an intuitive way we consider it as a generalization of probability theory, which provides a way to represent hesitation and ignorance indifferently.

5.1. Track elements degradation measure

The characteristics of sensors vary in their ability to detect information that is relevant to the fault detection task and decision making. Two conditions apply when estimating the nonlinear characteristics of the component degradation measure: *exhaustive and mutual exclusion of faults and sensor weighting*. Regarding the information provided by two sensors, suppose that the propulsion engine suffers from two faults: α_1, "*fault of injection valve*", *and* α_2, "*engine temperature fault*." The mass functions associated with these two sensors are respectively f_{m1} and f_{m2}. As the objective is to perform fault diagnosis with regard to a specific sensor, the frame of discernment in this case can be set as $U = \{\alpha_1, \alpha_2\}$ and $\Gamma(\aleph) = \{\alpha_1, \alpha_2, \{\alpha_1, \alpha_2\}\}$. Because neither is present, $f_{m1}(\{\alpha_1, \alpha_2\}) = 0$ and $f_{m2}(\{\alpha_1, \alpha_2\}) = 0$.

Typically, a sensor's sensitivity depends on the true source location as well as the sensor's location. We define a weight vector to build up information about the influence of local behavior over the whole sensor network. In addition, to be independent of one another, only one fault is expected to occur at any given instance k (*mutual exclusion*). For the sake of simplicity, we consider risk to consist of two main factors: (1) the cost (or impact) $\varphi_{x_0}(x(t))$ of a damage, a crisis, a catastrophe, etc., in the state $x(t)$, knowing that $x_0(t)$ is the initial state; and (2) the likelihood $\hbar_{x_0}(x(t))$ that the damage will occur in the state $x(t)$, knowing that $x_0(t)$ is the initial state of the system. The synthesis of these factors can be used to express the generic measure of risk as follows:

$$\forall t \geq 0, \quad \rho_{x_0}(\xi(t)) = \int_0^T \hbar_{x_0}(x)\varphi_{x_0}(x)dt \tag{16}$$

Application of the evidence-based analysis of the above consideration shows that

$$\begin{cases} Bel_1(\{\alpha_1\}) = Pl_1(\{\alpha_1\}) = 0.12 \\ Bel_2(\{\alpha_2\}) = Pl_2(\{\alpha_2\}) = 0.88 \end{cases} \text{and} \begin{cases} Bel_2(\{\alpha_1\}) = Pl_2(\{\alpha_1\}) = 0.91 \\ Bel_2(\{\alpha_2\}) = Pl_2(\{\alpha_2\}) = 0.09 \end{cases} \tag{17}$$

This simple example reveals that both faults α_1 and α_2 exist and is evidence of two opposing conclusions because we assume mutually exclusive faults.

As a result, we establish affirmative evidence that should directly support the assertion to a certain degree and provide no support for its negation. The fuzzy isolation scheme and the decision-making rule that helps sustain the affirmative evidence are summarized as follows:

(1) build the membership functions $\mu_{\varepsilon ij}$ for each fault $i = 1, ..., n$, and for each sensor $j = 1, ..., m$,
(2) define the threshold value and the number of consecutive time instants t_k to isolate a fault,
(3) calculate the distance d_{ki} (9) and all of the fuzzy decision factors,
(4) determine the maximum belief function and the minimum belief interval, and
(5) compare the decision factors with the threshold
(6) until the maximum support and plausibility rule (14), the hypothesis with maximum belief function, is satisfied.

If one thinks of the system χ_1 as a power transmission system and system χ_2 as an information communications system, the meaning and effect of the coupling is fairly clear. The two systems are coupled in both directions. Outages (failures) in these systems can grow and evolve in non-uniform clusters and display a remarkably rich variety of spatial and temporal complexity. They can grow to all sizes, from individual node failures to system size events that may affect public safety.

We assume that risk is modeled in these systems by a random variable $\xi(t)$ (16), which represents the uncertain gains (or losses if negative) of a decision. In addition, $\rho : \xi(t) \mapsto \rho(\xi(t))$ is a risk measure functional in the random state $x(t)$ under the dynamics $x'(t) \in F(x(t))$, as defined in Eq. (3). The following section provides the ability to model a large amount of decision problems, particularly for risk management and situation awareness. It presents a short case study for propulsion cooling system risk analysis and health monitoring of a vessel.

6. Application example

The purpose of this section is to validate the obtained advanced intuitionistic fuzzy sets in the advanced framework of the Dempster–Shafer theory of evidence results through their application to monitoring the health of propulsion engine systems. This application refers to a typical sensory problem: *how to react, facing ambiguous settings (information) expressed on the same subject (*i.e., *system state metrics) using various sensors, where distortion causes can affect not only the sensing process mean and variability but also the correlation both among sensory variables and physical interference features*. A test program was conducted using a six-cylinder Hitachi-Man-B&W 6L80MC/MCE main engine. The engine pressure experimental data at a range of engine speeds and loads was collected and compared to experimental results.

Details of the ship engine geometry and operating conditions are given in Appendix A.2. The engine coolant was a one-to-one volume solution of ethylene glycol and water. Because the engine heat release rate is the best indicator to predict engine performance and efficiency, a heat-release test was carried out, and the chamber pressure data during a complete engine cycle was obtained. The pressures in the combustion chamber of the engine were measured by a series of four water-cooled, AVL piezoelectric pressure transducers. These transducers were mounted in the midplane of the trochoid housing in such a way that the pressure in a chamber of interest would constantly be monitored.

Moreover, pressure sensors were mounted at different locations on pumps interconnected to the primary sea water-cooling system of a ship engine. To maintain a sufficient cooling capacity in the ship engine, two charge pumps and two-stage compressors were supplied. As a result, the initial rated capacity of the pump of 1075 gpm could be increased to 1380 gpm. Pumps were supplied with a 690-gpm flow rate through each pump. The coolant flow was measured by a turbine flowmeter during harbor stays. Through this period, while the main engine of the ship was shut down, the cooling flow rate was reduced. However, the sensor (s_2) on pump (1) indicated that the pump was producing a discharge pressure of 1816.4 psig, which was higher than the pump's discharge line design pressure of 1794 psig. Table 1 shows the state vectors of the compressors, the heat exchanger, and pumps.

Table 1
Cooling system features sensed from three sensors.

	Sensors (s_1)		Sensors (s_2)		Sensors (s_3)	
	C. low pressure (psi)	C. high pressure (psi)	Pump (l) (psi)	Pump (2) (psi)	Leakage Int. (Lt/min)	Leakage line (Lt/min)
x_0	126.855	142.382	1552.73	1552.73	0.012	0.021
x_1	127.734	145.605	1587.10	1577.72	0.113	0.098
x_2	130.957	146.121	1723.43	1622.97	0.172	0.121
x_3	129.885	147.949	1816.40	1620.68	1.314	0.153

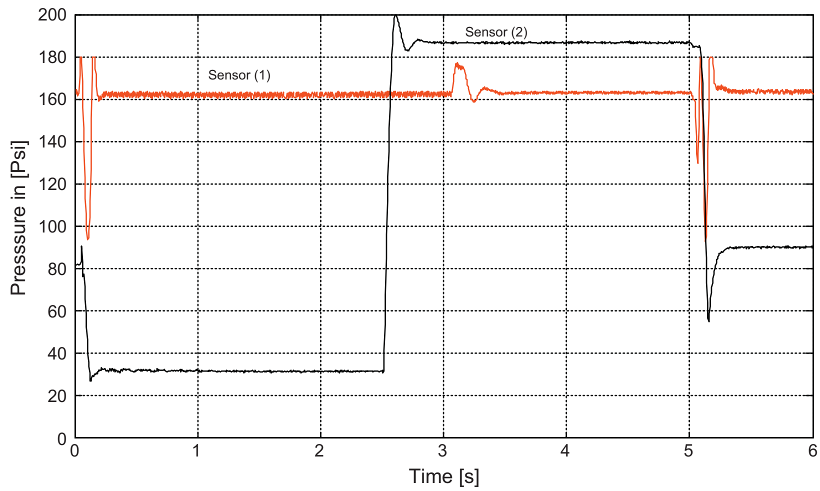

(a) Sensor (1) and (2) data inconsistency

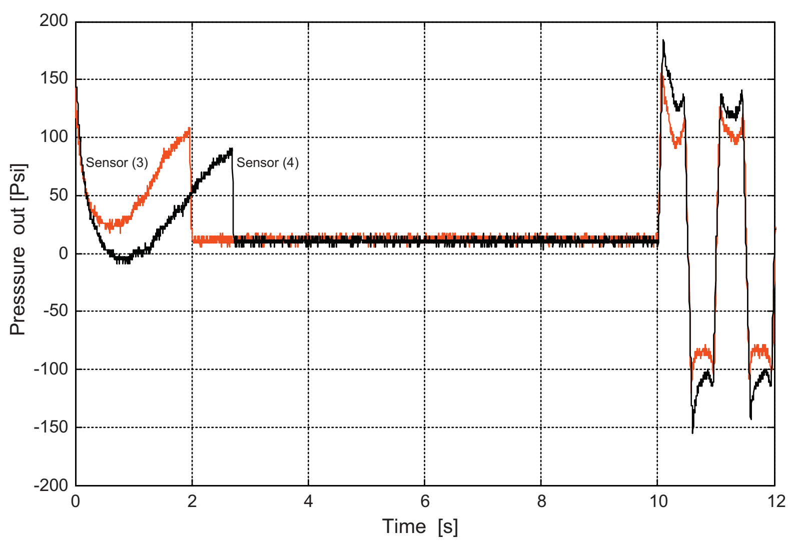

(b) Sensor (3) and (4) data inconsistency

Fig. 7. (a)–(b) Pressure in sensors errors.

The following section discusses the analysis sensor sensitivity regarding the integrity and the quality of measured data. The analysis should provide sufficient knowledge for achieving a better estimation of the cooling system states. Fig. 7(a) and (b) depicts the resulting fault symptoms from pumps and compressors provided by multiple sensors data. The figures illustrate that there is loss of linear independence between sensors. Pressure sensors (s_1) and (s_2) exhibit no correlation in space or time. The data indicate that the transient patterns appear more frequently from the running-in stage to the failure stage, which corresponds to the deterioration of the cooling performance as shown in Table 2. A cross-correlation-based analysis shows an instantaneous and large pressure shift and a time delay between sensors (s_5) and (s_6) responses presented in Fig. 8.

Table 2
Performance accuracy of fault diagnosis with combination of sensors set.

	Sensors (s_1)	Sensors (s_2)	Sensors (s_3)	Sensors $\sum_{i=1}^{2} S_i$	Sensors $\sum_{i=1}^{3} S_i$
Accuracy [%]	83.4	81	82.7	89.3	94.6

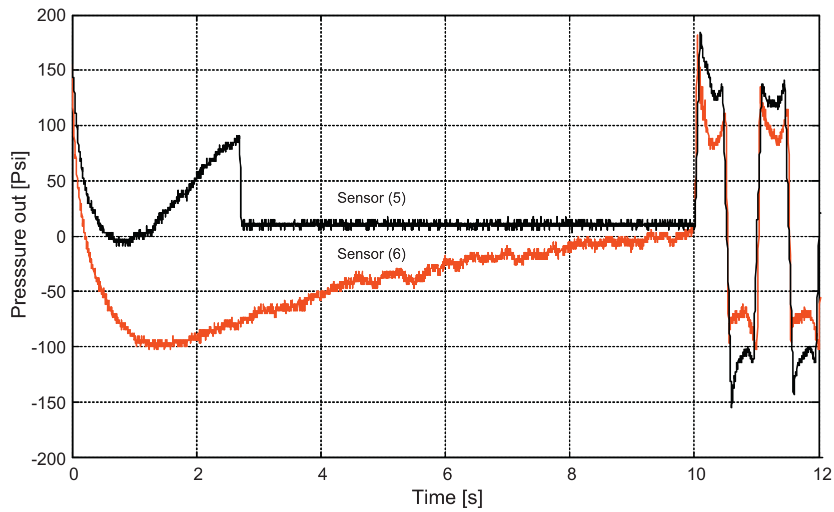

Fig. 8. Pressure out distortion; sensors (5) and (6) errors.

Fig. 8 shows that the time-domain signals originating from sensors strongly dephase (decay). Because the dephasing relies on dipolar coupling phenomena, anything that may reduce this can result in signals that are not properly suppressed. Such intervention can leave large, uncorrectable phase distortions in the data spectrum.

Obviously, the robustness of a sensor's sensitivity determines the existence of large interferences between sensors during engine health monitoring. We concluded that these measurements did not provide very credible information from which to make unbiased safety decisions. Therefore, we should evaluate the uncertainty in sensors dynamics by calculating the belief values. The next step is to use the proposed method to convert the information contained in the log-likelihoods into the evidential formalism so that corresponding information from the data fusion and decision-making features are usable. Because information about the system's state provided by sensors is critical for decision making, the analysis of the proportion of belief, which is associated with the union of the aforementioned hypotheses, enables us to decide whether real-time sensor fault detection and classification is certain or error prone.

Assume that sensors are equally sensitive to the system's states. However, their position may not be precisely known (calibrated). Also, signal wave front distortions due to random inhomogeneities of the medium are related to perturbations in sensor position. The fault frame of discernment in this case is $\aleph = \{x_0, x_1, x_2, x_3\}$. Because the system's state matrix X and the set $\aleph$ are determined, the evidence-theory-based formulation method can be easily implemented. The mass function (14) is slightly modified to reflect the sensor's capability by weighting the probability scheme. The weights are all set to 0.25. Table A2 depicts the relative values for the accuracy rates based on midrange values of failure rates found in commercially available systems. A literature review was used to determine the mean time to repair (MTTR) values for the main components as well as the onboard or onshore repair possibility of the propulsion pod unit shown in Table A2 (Appendix A.2), (Aksu and Turan, 2007).

The decision to act is initiated based on Eq. (16). The threshold is set-based on the knowledge of the system because it defines the regions of fault and no fault. These values can suffer slight changes in other processes. From Eq. (9), several distances d_{ki} can be above the threshold at a certain time k. Therefore, the ith fault is isolated only when the remaining faults are below the threshold. Because we assumed that only one fault may cross over the admissible threshold at a certain time instant k due to noise or interference errors, our approach considers the entropy of evidence E_m from the mass function f_m to quantify the information from a combination of pieces of evidence as follows:

$$E_m = \prod_{A \subset \aleph} [Pl(A)]^{f_m(A)} = \prod_{f_m(A) \neq 0} [Pl(A)]^{f_m(A)} \quad (18)$$

In this case where we combined the evidence, E_m reflects the performance of the set of sensors under the information fusion scheme. The complete combination procedure consists of n steps, where n is the element number of $\aleph$ (the number of diagnostic models); E_m satisfy the following:

$1/n \le E_m \le 1$ $E_m = 1/n$, if $f_m(\{\alpha_i\}) = 1/n$; $\alpha_i \in \aleph$, $i = 1, ..., n$; $E_m = 1$, if there exist two focal elements A_i and A_j such as $A_i \cap A_j = \varnothing$.

Combining (21) and (25), the calculated entropy evidence for sensor s_1 is $E_{m1} = 0.465$, while $E_{m2} = 0.386$.

The entropy evidence for the fused information E_{m12} and E_{m123} are 0.574 and 0.712, respectively. These values are very high and indicate considerable alterations in the associated dynamical parameters. Even though they did not yet reach the threshold and the failure propagation gains a value of 100%, which is defined as an irreversible phase transitions (i.e., catastrophic event), they did raise serious concerns about the engine health in critical operations. A convenient reference measure in this case was the "*triggering limit*," the size of a step failure that moves the center of the residual distribution to the threshold at a steady state. The entropy of the collected evidence synthesized the sources of the information fusion, thus leading to an enhancement in the prediction of the degradation trend of the engine performance. This evidence indicates the appearance of a new phase in the degradation of the engine performance.

7. Further research and development issues

The main goal of systems health monitoring and diagnostics is to make diagnostic decisions under conditions of uncertainty and imprecision. The multi-sensor fusion approach reviewed in this study is comparable to some of the early technology-based analogies and models of the brain based on intuitionistic fuzzy sets in the advanced framework of the Dempster–Shafer evidence theory. The human brain routinely carries out information gathering and fusion. Analogous to the human brain, the diagnostic and decision-making structure is used to evaluate the performance of multi-sensor data fusion applications to safety-critical systems (e.g., biomedical and nuclear systems, aircrafts) health monitoring. Losing control of its propulsion system in inclement sea causes a ship to experience diminished performance, lose stability, and possibly sink due to a complete loss of control. The results of this study provide some evidence regarding the application of the model and open avenues for the usefulness of the analogy and abstraction in brain science. The literature provides a comprehensive decision and control strategy that integrates probabilistic robust control, damage mitigating control, health and usage monitoring systems, and discrete event supervisory decision and control. A fuzzy model reference learning controller was used to reconfigure the nominal controller of an F-16 aircraft to compensate for actuator failures with and without explicit information about the failure.

In summary, the solutions to the safety problem in the commercial marine industry involve better system and organizational management as well as improved safety regulation and enforcement. The risk-assessment model developed herein is an important building block in the development and assessment of management and decision-making options related to ships' safety. Specific measures may include the following: (a) rational review of the existing safety techniques in the context of formal safety assessment and (b) novel ship safety assessment. Safety assessment techniques currently used in ship safety assessment need to be studied further, and the criteria for their effective use must be established in safety assessment.

8. Conclusion

The fault uncertainty tracking method for risk assessment based on fuzzy decision making proposed in this paper is developed from a holistic point of view and can be applied to both abrupt and incipient faults. Even though the fault frame of discernment techniques is implemented to determine a holistic view of the system behavior and faults impacts, the study and evaluation of the fuzzy-model-based diagnostic is much more difficult to implement as a decision-making tool. However, as a matter of fact, the proposed fuzzy logic monitoring tool exhibits the kinds of reliable characteristics that enable implementing rational diagnosis decision-making rules. More importantly, although the availability of an accurate diagnostic model should not be a precondition of a good control design, this study demonstrates how the accuracy of the fault diagnosis can be improved by fusing information from multiple sensors. The determination of the minimum number of sensors is associated with the cost of processing online, the initial placement of sensors, and other equipment criteria that are not considered here. Even though the modeling technique is developed with a holistic view of fault configuration effects, the study and evaluation of ship engine assessment as a decision-making tool is beyond the scope of this paper.

Acknowledgments

The present work was performed within the scope of the activities of the Small Grant project. The financial support of the University of Minnesota, Chancellor's Faculty Small Grant FY 2008 is gratefully acknowledged.

Appendix A.

A.1. Mathematical Model of the Motor Torque

$$\begin{cases} T = J\dfrac{d}{dt}\omega_{rm} + \beta\omega_{rm} + k_m{\omega_{rm}}^2 + T_d \\ T_d = \begin{cases} \alpha(\omega_{rm} - \omega_{cav})^2, & \omega_{rm} \geq \omega_{cav} \\ 0, & \omega_{rm} < \omega_{cav} \end{cases} \end{cases} \tag{A1}$$

where T is the motor torque [Nm], J is the equivalent inertia [kg m^2], ω_{rm} is the angular speed of the motor [rad/s], β is the friction coefficient [Nm/(rad/s)], k_m is the coefficient of the term related to the thrust [Nm/(rad/s)^2], T_d is the disturbance torque due to cavitation [Nm], ω_{cav} is the critical speed for which thrust loss occurs, and α

Table A1
Coefficients of the engine model.

φ_1 = 3294.01	φ_2 = 3059.7	φ_3 = 6.63
φ_4 = 20686.02	k_p = 1.18	Clean hull
Ship characteristics: ship draft = 5.86 m		
Engine power	19, 863.00 kW	Wave 0
Engine speed	93.4 rpm	Wind 2
Ship speed	21.208 knot	Ocean current

Table A2
MTTR data for the main components of the propulsion pod.

Steerable pod unit	Component	Sub-component	MTTR (h)	Repair onboard	Repair onshore
Thrust equipment	Electrical Motor	Rotor	500		X
		Stator	500		X
		Bearings	16		X
		Temperature sensor	10		
	Converters	Power components	2	X	
		Control system	2	X	
		Cooling system	50		X
	Shaft	Propeller bearings	16		X
		Thrust bearings	16		X
	Draining system	Pumps and piping	3		X
	Propeller or hub seals		8		X
	Propeller assembly				
Steering & thrust equip.	Cooling system	Heat exchanger	1	X	
	Lubricating system	Cooling system pumps and piping	3	X	
		Lubricating system pumps and piping	3	X	
		Lubricating system filters	1	X	
Steering equipment	Air drying system		2	X	
	Hull or axis seals		8		X
	Hydraulic power pack		4	X	
	Hydraulic motor		3	X	
	Driving gears		3	X	X
	Journal bearings		6		X

is a certain coefficient. Assume the frame of discernment is defined as follows:

$$\aleph = \{\varepsilon_0, \varepsilon_1, \varepsilon_2, .., \varepsilon_{h-1}, \varepsilon_h\} \tag{A2}$$

These parameters remarkably vary according to the environmental and seaway conditions. The motor position error could be expressed as follows:

$$\begin{cases} e_\theta(t) = \theta_r(t) - \theta(t) \\ \varepsilon_\theta(t) = \dot{e}_\theta(t) + k_p e_\theta(t) + k_i \displaystyle\int e_\theta(t)dt \end{cases} \tag{A3}$$

Another way to formulate the dynamic of the position error is:

$$\dot{\varepsilon}_\theta(t) = \frac{1}{J}\left[-T(t) - \beta\varepsilon_\theta(t) + h(x, \upsilon)\right] \tag{A4}$$

where $h(x, \upsilon)$ is the approximation error term, $\theta_r(t)$ is the reference position signal, x is the state vector and υ the vector of the uncertainty, $e_\theta(t)$ is the position error.

The control signal of the speed controller is formulated such that

$$\begin{cases} u = h(x, \upsilon) - T \\ x = \left[\displaystyle\int e_\theta(t)dt, \quad e_\theta(t), \quad \dot{e}_\theta(t), \quad \ddot{e}_\theta(t)\right]^T \end{cases} \tag{A5}$$

While requirements in Eq. (A5) may broadly apply because of the involvement of human (expert) judgment in the overall control loop for the interpretation of data and observations, the uncertainties become an integral part of the decision-making process related to suspicious information from sensors.

A.2. Ship Engine Technical Parameters

The model of the Hitachi-Man-B&W 6L80MC/MCE main engine used in this study was a six-cylinder, two-stroke, low-speed marine diesel engine, which was fitted with two VTR-564-32 exhaust gas turbochargers with a rated speed of 88 rpm, rated power of 16,668.00 kW, and stable speed of 12,280.00 rpm used to increase the air pressure. Coefficients φ_i, $i = 1, ..., 4$ and k_p in Eq. (9) are given below:

Table A1.

A.3. The Mean Time to Repair

Table A2.

References

Abou, S.C., 2010. Performance assessment of multi-state systems with critical failure modes: application to the flotation metallic arsenic circuit. Reliability Engineering & System Safety 95 (6), 614–622.

Abou, S.C., Lu, C., Saad, M., 2007. Advanced diagnostic/prognostic system: an integrated approach to systems health monitoring. In: ATRS, World Conference, Berkeley, CA.

Aksu, S.K., Turan, O., 2007. Quantitative reliability and availability analysis for design evaluation of generic pod propulsion systems. Journal of Risk and Reliability 221 (1), 13–28.

Alfaro-Cid, E., McGookin, E.W., Murray-Smith, D.G., 2001. Genetic algorithm optimisation of a supply ship propulsion and navigation systems. Oceans Conference Record, IEEE 4, 2645–2652.

Atanassov, K., 1999. Intuitionistic Fuzzy Sets: Theory and applications. Springer-Verlag, New York.

Barnett, J.A., 1981. Computational methods for a mathematical theory of evidence. Proc. IJCAI, 868–875.

Benitez-Perez, H., Quinones-Reyes, P., et al., 2006. Reconfigurable fuzzy Takagi Sugeno networked control for magnetic levitation case study Mexican International Conference on Artificial Intelligence. Lecture Notes on Computer Science, 134–145.

Carter, R.L., Geib, C.W., et al., 2001. Information modeling for intrusion report aggregation. In: DISCEX-II Conference, pp. 329–342.

Elishakoff, I., 2004. Safety Factors and Reliability: Friends or foes? Springer, New York, ISBN 1402017790.

Gabasov, R., Kirillova, F.M., 2006. Real-time optimal control and observation. Journal of Computer and Systems Sciences International 45 (3), 421–441.

Groenen, P.J., Jajuga, K., 2001. Fuzzy clustering with squared Minkowski distances. Fuzzy Sets and Systems 120 (3), 227–237.

Haimes, Y.Y., 2004. Risk modeling, Assessment and Management, 2nd ed. John Wiley & Sons, New Jersey.

Harvald, S.A., 1983. Resistance and propulsion of ship. John Wiley & Sons.

Henley, E.J., Kumamoto, H., 1980. Reliability Engineering and Risk Assessment. Prentice-Hall, Englewood Cliffs, N.J.

Holtrop, J., 1984. A statistical reanalysis of resistance and propulsion data. International Shipbuilding Progress 31, 272–276.

Kahneman, D. (2002, Dec. 8). Maps of bounded rationality: a perspective on intuitive judgment and choice. [Nobel Prize Lecture].

Lisnianski, A., Levitin, G., Ben-Haim, Y., 2000. Structure optimization of multi-state system with time redundancy. Reliability Engineering & System Safety 67 (2), 103–112.

Murchland, J., 1975. Fundamental concepts and relations for reliability analysis of multi-state systems and fault tree analysis. Theoretical and Applied Aspects of System Reliability, SIAM, 581–618.

Safranek, R.J., Gottschlich, S., et al., 1990. Evidence accumulation using binary frames of discernment for verification vision. IEEE Transactions on Robotics and Automation 6 (4).

Sauer, T., Yorke, J.A., Casdagli, M., 1991. Embedology. Journal of Statistical Physics 65, 579–616.

Shafer, G., 1976. A Mathematical Theory of Evidence. Princeton University Press, N.J.

Sugeno, M., 1974. Theory of Fuzzy Integrals and its applications. Tokyo Institute of Technology, Japan.

Szmidt, E., Baldwin, J., 2003. New similarity measure for intuitionistic fuzzy set theory and mass assignment theory. Notes on IFS 9 (3), 60–76.

Szmidt, E., Kacprzyk, J., 1996. Intuitionistic fuzzy sets in group decision making. Notes on IFS 2, 15–32.

Szmidt, E., Kacprzyk, J., 2005. A new concept of a similarity measure for intuitionistic fuzzy sets and its use in group decision making. Springer, New York, pp. 272–282.

Wang, J., Yang, J.B., Send, P., 1995. Safety analysis and synthesis using fuzzy set modeling and evidential reasoning. Reliability Engineering & System Safety 47 (3), 10–118.

Yager, R.R., 1983. Entropy end specificity in a mathematical theory of evidence. International Journal of General Systems 9, 249–260.

Yager, R.R., Kacprzyk, J., et al., 1994. Advances in the Dempster-Shafer Theory of Evidence. John Wiley & Sons, Inc., New York.